Neutron resonance spectroscopy. XVI. ^{113}In, ^{115}In†

G. Hacken, H. I. Liou, H. S. Camarda,* W. J. Makofske, F. Rahn,‡
J. Rainwater, M. Slagowitz,§ and S. Wynchank‖
Columbia University, New York, New York 10027
(Received 10 June 1974)

Results of neutron time of flight spectroscopy measurements for natural indium and separated ^{115}In, using the Nevis synchrocyclotron, are given. Transmission and self-indication measurements were made for a range of natural indium sample thicknesses and for a sample of 99.5% enriched $^{115}In_2O_3$. Resonance parameters E_0 and $g\Gamma_n^0$ are given to 2 keV. Part of the isotope assignment was made with the aid of ^{113}In raw capture data taken at Geel by C. Coceva. Some Γ_γ values were also obtained, from which we estimate $\langle\Gamma_\gamma\rangle$ to be 75 meV for ^{113}In (based on three levels), and 85 meV for ^{115}In (15 levels). The $l=0$ strength function for ^{115}In is $10^4S_0=0.26\pm0.03$. Comparison of the $(g\Gamma_n^0)^{1/2}$ distribution with Porter-Thomas theory for ^{115}In shows that many p levels are observed. An estimate of the level detection sensitivity and a Bayes's theorem analysis allow a determination of the p strength function and its uncertainty: $10^4S_1=2.7+1.0$ or -0.7 for ^{115}In. We find $\langle D\rangle=(9.4\pm0.2)$eV for ^{115}In s levels.

[NUCLEAR REACTIONS $^{113,115}In$ (n,n), (n,γ), $E=0-2$ keV; measured σ_t (E); deduced E_0, $g\Gamma_n$, Γ_γ, S_0, $\langle D_0\rangle$, S_1.]

I. INTRODUCTION

This paper is one of a series[1-8] reporting results of high resolution pulsed neutron time of flight spectroscopy using the Columbia University Nevis synchrocyclotron as a source. Results are presented for measurements using one sample of separated ^{115}In (99.5% ^{115}In) in the form of In_2O_3, and several sample thicknesses of natural indium metal (95.72% ^{115}In, 4.28% ^{113}In). The measurements included transmission measurements using our 202.05 m flight path in conjunction with a neutron time of flight (TOF) system having 8192 timing channels. The highest resolution transmission runs used 50 ns TOF channel widths for neutron energies >1.6 keV and 100 ns widths for 0.68 to 1.6 keV. Other transmission runs covered the energy range 20 eV to 2.3 keV, with channel widths decreasing (in blocks of 512 channels) from 800 ns at low energies to 100 ns above 0.79 keV.

In addition to transmission measurements, self-indication measurements were made using a 39.57 m flight path and the same TOF system. The self-indication detector counted capture γ rays from an indium sample placed at the detector (D) position. A particular experimental run either had an additional indium sample at the transmission (T) position, called ("$D+T$"), or did not ("D only"). Methods of data analysis used to determine resonance parameters from observed capture peaks ("D only" and "$D+T$") and transmission dips (200 m detector) are described in earlier papers of this series.

Prior to these measurements, level parameters had been presented for seven levels in ^{113}In to 46 eV, and 11 levels in ^{115}In to 95 eV in BNL 325. Harvey *et al.*[9] give values for six more levels in ^{113}In to 105 eV in addition to six levels to 46 eV. Sailor and Borst[9] measured the first level in ^{113}In at 1.8 eV and a few more to 26 eV. The earlier ^{115}In results were also mainly those of Harvey *et al.*[9] except for the level at 1.456 eV, for which many groups measured the parameters. While level structure is seen in our present data to energies $\gg 2$ keV, the level density is such that a cutoff at 2004 eV was made in the level parameter analysis for ^{115}In and ^{113}In. Since we did not use an enriched ^{113}In sample, part of the 282 levels seen using the natural In samples ($1/n=10.04$, 29.5, and 336 b/atom) were classified as ^{115}In levels if they were among the 182 levels observed for the enriched ^{115}In sample ($1/n=704$ b/atom). Since the thickest natural In sample is expected to reveal many weak ^{115}In levels not detected in the (thin) enriched ^{115}In sample (in addition to our total observed set of ^{113}In levels), extra tests were needed to assign these levels to ^{113}In or ^{115}In. Assignment as ^{113}In levels was made for those levels seen in natural In of such strength that they should have been observed in the enriched ^{115}In sample if they were ^{115}In levels. There were 34 levels in this category. This leaves 66 levels in natural In not covered by these tests. Fortunately, Coceva informed us that he had made time of flight capture measurements at Geel using an enriched sample of ^{113}In and a sample of natural In.[10] A subsequent interchange of preliminary results helped to permit assignment of our extra 66 levels seen in natural In to ^{113}In or ^{115}In. Coceva's data were not analyzed for level parameters, but he has reported some results[11] of an analysis of the capture intensity distribution for ^{115}In levels using our preliminary $g\Gamma_n^0$ assignments. Coceva's ^{113}In level listing was to 2002 eV so that we believe that our final isotope assignments to 2004 eV are correct. While we include all but very weak ^{115}In s levels, our ^{113}In level set is quite incomplete due to masking of ^{113}In in natural In by levels due to the main abundance ^{115}In isotope.

We obtain the level energy E_0 and $g\Gamma_n^0$ value for each of our observed levels. Since both isotopes have $I=\frac{9}{2}$, the g factors for $l=0$ levels are either $\frac{9}{20}$ or $\frac{11}{20}$, which are too nearly the same to allow us to assign J values to individual levels. In some favorable cases, we are able to establish the level capture width Γ_γ. The binding energy of an extra neutron is 7.31 MeV for ^{113}In and 6.62 MeV for ^{115}In.

Indium occurs at a minimum in the strength function $S_0=\langle g\Gamma_n^0\rangle/\langle D\rangle$ for $l=0$ resonances, but at the high end of a (split) maximum for the strength function S_1 for p levels. A comparison of observed distribution of $g\Gamma_n^0$ values for ^{115}In with the single channel Porter-Thomas distribution shows that we have an excess of weak levels, mainly below 500 eV, which are probably due to an inclusion of the larger levels of the p-wave distribution. From our detection sensitivity and the stronger portion of the observed $g\Gamma_n^0$ distribution, we can estimate the likely number of missed s levels and included p levels vs the assumed value of S_1. This permits a determination of both S_0 and S_1, as well as the proper choice of the corrected mean $l=0$ level spacing. The results of further statistical tests are also presented.

The analysis of the In data is mainly due to G. Hacken as part of his Ph.D. thesis.

II. EXPERIMENTAL CONDITIONS

The In measurements were made at the same time as those for the Er and Yb isotopes.[1,4] The natural In metal samples were 7.5×22.5 cm area. The enriched ^{115}In sample, in the form of In_2O_3, 7×24 cm area, was mainly intended for use with the 39.57 m capture detector which is more sensitive for detecting weak levels than a transmission detector. About 1.6×10^6 cyclotron bursts, at 60/sec, of counting time was spent on the ^{115}In sample "D only" leading to $>2\times10^4$ counts/channel at the peak for the 9 eV level where the background is ~2000/channel (400 ns channel width). About 6.4×10^6 cyclotron bursts were used for the natural In sample self-indication measurements. About 2×10^6 bursts were used for the natural In 200 m transmission measurements which proved to be useful in the analysis. The total count rate was ~40/burst below 2 keV for a thin sample.

A spectroscopic analysis for the natural In samples showed <0.01% for any impurity which might be responsible for any of our observed levels. No levels were seen at the position of strong levels for elements present at $\leq 0.00x$% abundance. We thus believe that none of our levels are due to other elements.

III. DATA ANALYSIS AND RESULTS

The methods of data analysis are the same as those described[1] for the Er isotopes. For each resonance seen with each sample thickness in transmission or in self-indication, a curve is obtained giving possible values of $g\Gamma_n$ vs Γ which match the observed level dip or peak. The intersection of these curves gave the favored $g\Gamma_n^0$ and Γ for the resonance. As many as eight such curves having a tight intersection region were obtained for some of the lower energy levels in ^{115}In, while a

TABLE I. Resonance parameters for ^{113}In. Levels labeled N are classified as ^{113}In because they are too strong to have been missed in our separated ^{115}In data if they were ^{115}In resonances. Levels identified as due to ^{113}In by Coceva or from his ^{113}In data are labeled G. All levels in this table and in Table II were observed in our natural indium data, except for the first level of each table, which was taken from Ref. 13.

E_0 (eV)	$g\Gamma_n^0$ (meV)	E_0 (eV)	$g\Gamma_n^0$ (meV)	E_0 (eV)	$g\Gamma_n^0$ (meV)	E_0 (eV)	$g\Gamma_n^0$ (meV)
1.80 ± 0.03	< .08	G123.4 ± 0.1	0.5 ± 0.1	NG511.6 ± 0.3	0.87 ± 0.10	NG 912.0 ± 0.4	3.0 ± 0.4
N 4.70 ± 0.03	0.032 ± 0.005	NG203.4 ± 0.2	1.33 ± 0.07	NG544.8 ± 0.3	1.8 ± 0.1	NG1064.6 ± 0.5	0.7 ± 0.1
N 14.65 ± 0.04	0.75 ± 0.25	NG228.5 ± 0.2	1.2 ± 0.3	NG555.4 ± 0.4	0.50 ± 0.05	G1230.0 ± 0.6	1.6 ± 0.2
NG 21.55 ± 0.01	0.30 ± 0.02	NG234.5 ± 0.2	0.42 ± 0.04	NG582.9 ± 0.4	2.3 ± 0.1	NG1254.6 ± 0.6	1.7 ± 0.2
NG 24.99 ± 0.01	0.93 ± 0.02	NG236.1 ± 0.2	0.22 ± 0.06	NG593.0 ± 0.4	0.85 ± 0.05	G1729.7 ± 1.0	0.5 ± 0.1
G 26.78 ± 0.02	0.020 ± 0.005	N 239.3 ± 0.2	0.19 ± 0.06	NG625.5 ± 0.4	1.4 ± 0.1	G1761.9 ± 1.0	1.5 ± 0.3
NG 32.24 ± 0.02	0.67 ± 0.04	NG241.7 ± 0.2	0.53 ± 0.06	NG660.8 ± 0.5	1.44 ± 0.09	G1872.9 ± 1.1	1.8 ± 0.3
NG 44.71 ± 0.03	0.15 ± 0.02	G270.5 ± 0.1	0.27 ± 0.04	NG714.6 ± 0.5	1.7 ± 0.2	G1885.2 ± 1.1	0.5 ± 0.1
NG 45.38 ± 0.04	0.125 ± 0.005	NG276.8 ± 0.1	0.10 ± 0.04	NG769.9 ± 0.6	1.3 ± 0.1	G1911.8 ± 1.1	1.14 ± 0.22
NG 70.29 ± 0.04	0.45 ± 0.03	G304.3 ± 0.1	0.36 ± 0.04	G777.6 ± 0.6	0.57 ± 0.05	G1974.0 ± 1.2	0.86 ± 0.25
NG 91.59 ± 0.04	1.57 ± 0.55	NG313.9 ± 0.2	0.20 ± 0.05	NG785.3 ± 0.6	0.73 ± 0.05	G1988.4 ± 1.2	0.56 ± 0.20
NG 93.00 ± 0.05	0.22 ± 0.02	NG325.8 ± 0.2	0.32 ± 0.06	NG809.4 ± 0.6	0.67 ± 0.05	G1996.0 ± 1.2	0.6 ± 0.2
NG103.95 ± 0.05	1.5 ± 0.1	G441.4 ± 0.3	0.33 ± 0.04				

single curve, along with the requirement $\Gamma \approx 2g\Gamma_n + \langle \Gamma_\gamma \rangle$ determined $g\Gamma_n^0$ for many weak levels, particularly above 1 keV. Since the plots are very similar to those[1] for the Er isotopes, examples have not been included here. At lower energies, partial shape fits were made to the data.

The final resulting sets of level energies and $g\Gamma_n^0$ values for ^{113}In and ^{115}In are given in Tables I and II. Preliminary results were given in Refs. 12 and 13. The isotope identification basis is given by the symbols before the energy. In each case, the level was observed for our natural In samples. Levels seen in our enriched ^{115}In sample have N before the energy. Levels seen in natural In, but not in Coceva's ^{113}In data are denoted by G in Table II. Levels seen in our natural In data where the levels are classified as ^{113}In because they are too strong to have been missed for our ^{115}In sample if

TABLE II. Resonance parameters for ^{115}In. Levels labeled N were seen in our ^{115}In separated isotope self-indication data. Those labeled G were seen in natural indium self-indication but not in Coceva's ^{113}In capture data. Below 500 eV, those marked with an asterisk are believed likely to be *p* levels on the basis of a Bayes's theorem analysis. The first level is taken from Ref. 13.

E_0 (eV)	$g\Gamma_n^0$ (meV)	E_0 (eV)	$g\Gamma_n^0$ (meV)	E_0 (eV)	$g\Gamma_n^0$ (meV)	E_0 (eV)	$g\Gamma_n^0$ (meV)
1.457 ± 0.002	1.38 ± 0.02	NG 379.1 ± 0.2	0.016 ± 0.003	NG 819.4 ± 0.3	0.15 ± 0.02	NG1389.3 ± 0.7	0.14 ± 0.01
N 3.85 ± 0.01	0.086 ± 0.008	NG 383.0 ± 0.2	0.03 ± 0.01	NG 829.8 ± 0.3	0.19 ± 0.01	NG1397.9 ± 0.7	0.17 ± 0.02
N 9.04 ± 0.03	0.27 ± 0.03	NG 384.2 ± 0.2	0.15 ± 0.02	NG 836.7 ± 0.3	0.31 ± 0.02	NG1402.1 ± 0.7	0.10 ± 0.01
N 12.02 ± 0.04	0.016 ± 0.001	NG 402.3 ± 0.2	0.78 ± 0.16	NG 853.5 ± 0.3	1.00 ± 0.07	NG1415.9 ± 0.7	0.33 ± 0.03
NG 22.73 ± 0.01	0.107 ± 0.004	NG 411.6 ± 0.2	0.77 ± 0.15	NG 861.1 ± 0.3	0.39 ± 0.07	NG1421.0 ± 0.7	0.043 ± 0.020
N * 29.70 ± 0.02	0.0003 ± 0.0002	NG 423.0 ± 0.2	0.25 ± 0.03	NG 863.9 ± 0.3	0.32 ± 0.07	NG1430.6 ± 0.8	0.12 ± 0.01
NG 39.60 ± 0.03	0.33 ± 0.02	NG*431.2 ± 0.3	0.005 ± 0.003	G 869.4 ± 0.4	0.027 ± 0.014	NG1441.8 ± 0.8	0.038 ± 0.007
NG 46.36 ± 0.04	0.018 ± 0.001	NG 437.2 ± 0.3	0.025 ± 0.002	NG 875.1 ± 0.4	0.117 ± 0.007	G1448.6 ± 0.8	0.041 ± 0.008
NG 48.14 ± 0.04	0.036 ± 0.007	NG 448.9 ± 0.3	0.30 ± 0.05	NG 882.6 ± 0.4	0.013 ± 0.007	G1460.7 ± 0.8	0.029 ± 0.015
NG 62.98 ± 0.03	0.047 ± 0.006	NG 453.9 ± 0.3	0.49 ± 0.10	NG 891.6 ± 0.4	0.266 ± 0.007	NG1468.4 ± 0.8	0.38 ± 0.06
NG 69.49 ± 0.03	0.024 ± 0.006	NG 456.8 ± 0.3	0.45 ± 0.05	NG 899.0 ± 0.4	0.059 ± 0.008	NG1480.0 ± 0.8	0.09 ± 0.01
G* 73.08 ± 0.04	0.0007 ± 0.0004	NG 469.6 ± 0.3	0.12 ± 0.02	NG 906.8 ± 0.4	0.010 ± 0.005	G1484.7 ± 0.8	0.007 ± 0.004
NG 80.87 ± 0.04	0.083 ± 0.006	NG*473.6 ± 0.3	0.013 ± 0.007	NG 913.9 ± 0.4	0.23 ± 0.01	NG1492.6 ± 0.8	0.056 ± 0.025
NG 83.28 ± 0.04	0.36 ± 0.04	NG 477.6 ± 0.3	0.072 ± 0.005	NG 923.4 ± 0.4	0.10 ± 0.03	NG1520.6 ± 0.8	0.56 ± 0.04
G* 86.36 ± 0.04	0.003 ± 0.002	G*488.0 ± 0.3	0.015 ± 0.005	NG 931.9 ± 0.4	0.037 ± 0.020	NG1546.1 ± 0.8	0.35 ± 0.04
NG 94.34 ± 0.05	0.15 ± 0.02	G*493.7 ± 0.3	0.011 ± 0.005	G 943.7 ± 0.4	0.018 ± 0.009	NG1554.4 ± 0.8	0.12 ± 0.06
NG*100.83 ± 0.05	0.002 ± 0.001	NG 498.2 ± 0.3	0.066 ± 0.005	NG 948.1 ± 0.4	0.85 ± 0.05	G1562.9 ± 0.8	0.063 ± 0.030
NG*110.90 ± 0.06	0.002 ± 0.001	G 501.9 ± 0.3	0.023 ± 0.008	NG 956.6 ± 0.4	0.51 ± 0.03	NG1567.1 ± 0.9	0.26 ± 0.03
NG 114.43 ± 0.06	0.005 ± 0.001	NG 503.7 ± 0.3	0.56 ± 0.09	G 973.8 ± 0.4	0.02 ± 0.01	NG1579.9 ± 0.9	0.038 ± 0.015
NG*120.71 ± 0.07	0.001 ± 0.001	NG 506.2 ± 0.3	0.024 ± 0.012	NG 978.0 ± 0.4	0.58 ± 0.03	NG1595.5 ± 0.9	0.39 ± 0.04
N *123.60 ± 0.07	0.001 ± 0.001	N 513.1 ± 0.3	0.004 ± 0.002	G 981.8 ± 0.4	0.046 ± 0.007	NG1614.0 ± 0.9	0.47 ± 0.05
NG 125.88 ± 0.08	0.17 ± 0.01	NG 515.4 ± 0.3	0.074 ± 0.005	NG 998.0 ± 0.4	0.53 ± 0.03	NG1619.3 ± 0.9	2.34 ± 0.26
NG 132.81 ± 0.08	0.23 ± 0.04	NG 525.5 ± 0.3	0.31 ± 0.05	NG1007.1 ± 0.4	0.013 ± 0.007	NG1640.9 ± 0.9	0.57 ± 0.03
NG 144.04 ± 0.09	0.006 ± 0.001	NG 530.1 ± 0.3	0.020 ± 0.002	NG1019.5 ± 0.4	0.014 ± 0.007	G1646.4 ± 0.9	0.030 ± 0.15
G*145.76 ± 0.09	0.0025 ± 0.0013	NG 547.9 ± 0.3	0.116 ± 0.005	NG1035.7 ± 0.5	0.11 ± 0.02	NG1654.7 ± 0.9	0.029 ± 0.15
NG 150.3 ± 0.1	0.19 ± 0.01	NG 551.1 ± 0.4	0.035 ± 0.002	NG1043.0 ± 0.5	0.81 ± 0.06	NG1663.9 ± 0.9	1.35 ± 0.20
G*158.6 ± 0.1	0.006 ± 0.004	G 559.7 ± 0.4	0.013 ± 0.007	NG1049.1 ± 0.5	0.081 ± 0.010	G1676.3 ± 0.9	0.032 ± 0.010
G*162.4 ± 0.1	0.005 ± 0.003	NG 562.6 ± 0.4	0.020 ± 0.002	NG1055.1 ± 0.5	0.016 ± 0.008	NG1678.6 ± 0.9	0.15 ± 0.03
NG 164.7 ± 0.1	0.70 ± 0.04	G 569.6 ± 0.4	0.011 ± 0.006	NG1060.3 ± 0.5	0.20 ± 0.01	NG1688.6 ± 1.0	1.83 ± 0.17
NG 168.1 ± 0.1	0.081 ± 0.004	NG 571.9 ± 0.4	0.74 ± 0.05	NG1075.1 ± 0.5	0.54 ± 0.06	G1693.3 ± 1.0	0.073 ± 0.035
NG 174.1 ± 0.1	0.008 ± 0.004	NG 580.2 ± 0.4	0.16 ± 0.01	NG1085.8 ± 0.5	0.51 ± 0.03	G1704.6 ± 1.0	0.024 ± 0.012
NG 177.9 ± 0.1	0.11 ± 0.02	NG 589.1 ± 0.4	0.14 ± 0.01	NG1103.7 ± 0.5	0.02 ± 0.01	NG1711.6 ± 1.0	0.63 ± 0.07
NG 187.0 ± 0.1	0.73 ± 0.07	NG 602.2 ± 0.4	0.043 ± 0.009	NG1111.7 ± 0.5	0.197 ± 0.009	G1723.3 ± 1.0	0.096 ± 0.024
NG*192.2 ± 0.2	0.0017 ± 0.0009	G 610.0 ± 0.4	0.017 ± 0.001	NG1140.2 ± 0.5	0.28 ± 0.01	NG1736.1 ± 1.0	0.72 ± 0.12
G*194.5 ± 0.2	0.004 ± 0.002	NG 614.1 ± 0.4	0.76 ± 0.04	NG1170.3 ± 0.5	0.24 ± 0.03	G1739.6 ± 1.0	0.11 ± 0.04
G*198.8 ± 0.2	0.0026 ± 0.0015	NG 619.6 ± 0.4	0.34 ± 0.03	NG1179.7 ± 0.6	0.28 ± 0.01	NG1764.2 ± 1.0	0.071 ± 0.025
NG 205.6 ± 0.2	0.80 ± 0.20	NG 643.9 ± 0.5	0.095 ± 0.005	NG1188.0 ± 0.6	0.044 ± 0.020	NG1780.5 ± 1.0	0.071 ± 0.007
NG 211.9 ± 0.2	0.017 ± 0.003	NG 647.1 ± 0.5	0.073 ± 0.004	NG1190.8 ± 0.6	0.048 ± 0.006	NG1789.8 ± 1.0	0.035 ± 0.012
G*214.1 ± 0.2	0.006 ± 0.001	NG 654.8 ± 0.5	0.176 ± 0.007	NG1199.3 ± 0.6	0.012 ± 0.006	NG1797.1 ± 1.0	0.52 ± 0.05
NG 224.0 ± 0.2	1.07 ± 0.20	NG 674.0 ± 0.5	0.217 ± 0.005	NG1213.1 ± 0.6	0.69 ± 0.09	NG1808.6 ± 1.0	0.047 ± 0.007
NG 226.8 ± 0.2	0.044 ± 0.026	NG 683.2 ± 0.5	0.060 ± 0.005	NG1216.6 ± 0.6	0.14 ± 0.07	NG1813.9 ± 1.0	0.031 ± 0.009
G*246.7 ± 0.2	0.006 ± 0.004	NG 694.6 ± 0.5	0.079 ± 0.004	NG1224.2 ± 0.6	0.57 ± 0.06	G1826.7 ± 1.0	0.035 ± 0.012
NG 250.2 ± 0.2	1.9 ± 0.1	G 699.1 ± 0.5	0.023 ± 0.012	NG1237.8 ± 0.6	0.021 ± 0.010	G1830.9 ± 1.1	0.054 ± 0.005
NG 267.0 ± 0.1	0.12 ± 0.01	G 704.8 ± 0.5	0.043 ± 0.004	NG1243.1 ± 0.6	0.30 ± 0.03	NG1843.9 ± 1.1	0.093 ± 0.023
G*282.3 ± 0.1	0.006 ± 0.003	NG 707.8 ± 0.5	0.11 ± 0.02	G1270.1 ± 0.6	0.05 ± 0.03	NG1855.6 ± 1.1	0.58 ± 0.06
NG 288.9 ± 0.1	0.59 ± 0.06	NG 719.8 ± 0.5	0.058 ± 0.005	G1276.8 ± 0.6	0.077 ± 0.035	NG1865.8 ± 1.1	0.15 ± 0.02
NG 294.3 ± 0.1	1.3 ± 0.3	G 724.1 ± 0.5	0.018 ± 0.009	NG1281.2 ± 0.6	0.23 ± 0.01	NG1877.9 ± 1.1	0.076 ± 0.015
NG*302.5 ± 0.1	0.003 ± 0.001	NG 727.8 ± 0.5	0.062 ± 0.004	G1304.7 ± 0.6	0.025 ± 0.013	NG1891.4 ± 1.1	1.72 ± 0.23
N *304.3 ± 0.1	0.003 ± 0.002	NG 733.3 ± 0.5	0.228 ± 0.005	NG1309.3 ± 0.6	0.196 ± 0.009	NG1904.4 ± 1.1	0.16 ± 0.02
G*308.4 ± 0.1	0.004 ± 0.002	NG 752.7 ± 0.5	0.042 ± 0.004	G1325.0 ± 0.6	0.16 ± 0.06	NG1919.3 ± 1.1	0.46 ± 0.05
NG 319.5 ± 0.2	0.42 ± 0.03	G 760.1 ± 0.6	0.02 ± 0.01	NG1330.9 ± 0.7	0.18 ± 0.01	G1925.6 ± 1.1	0.032 ± 0.013
G*329.6 ± 0.2	0.006 ± 0.003	NG 774.0 ± 0.6	0.38 ± 0.04	NG1334.3 ± 0.7	0.11 ± 0.01	NG1939.6 ± 1.2	0.23 ± 0.02
G*336.7 ± 0.2	0.006 ± 0.003	NG 783.5 ± 0.6	0.284 ± 0.007	G1342.3 ± 0.7	0.11 ± 0.01	NG1948.4 ± 1.2	0.41 ± 0.02
NG 339.8 ± 0.2	0.052 ± 0.003	NG 789.6 ± 0.6	0.30 ± 0.02	G1346.0 ± 0.7	0.19 ± 0.01	NG1959.6 ± 1.2	0.45 ± 0.09
G*345.2 ± 0.2	0.008 ± 0.004	NG 795.1 ± 0.6	0.10 ± 0.07	NG1349.8 ± 0.7	0.40 ± 0.06	NG1968.6 ± 1.2	0.22 ± 0.05
NG 354.1 ± 0.2	0.17 ± 0.05	NG 800.6 ± 0.6	0.015 ± 0.08	NG1357.9 ± 0.7	0.099 ± 0.009	NG1981.8 ± 1.2	0.45 ± 0.05
NG 362.1 ± 0.2	0.29 ± 0.01	G 812.6 ± 0.6	0.009 ± 0.005	NG1367.6 ± 0.7	0.022 ± 0.010	G1992.7 ± 1.2	0.027 ± 0.014
G*366.9 ± 0.2	0.009 ± 0.003	NG 815.7 ± 0.6	0.059 ± 0.011	NG1372.4 ± 0.7	0.038 ± 0.020	N 2003.7 ± 1.2	0.20 ± 0.04
NG 370.9 ± 0.2	0.18 ± 0.01						

due to ^{115}In have N in Table I. Levels seen in our natural In data and identified as due to ^{113}In by Coceva have a G in Table I. Most of the levels included in Coceva's ^{113}In data were not seen in our data and are not included in Table I.

Not included in these tables are the Γ_γ values established for 3 levels in ^{113}In and 15 levels in ^{115}In. The $\langle\Gamma_\gamma\rangle$ values for ^{113}In and ^{115}In are 75 and 85 meV. Values for ^{113}In range from 70 to 80 meV. The mid $\frac{2}{3}$ of the values for ^{115}In range from 65 to 95 meV and are consistent with much smaller true fluctuations about $\langle\Gamma_\gamma\rangle$.

Figure 1 shows a plot to 500 eV of the many channel average cross section established using the transmission data for the $1/n = 10.04$ b/atom natural In sample. Many channel averages were used and regions very close to resonances were excluded so the plot would emphasize "between resonance" behavior. The observed fluctuations are almost entirely due to the effects of neighboring levels. The average value has $\sigma_{pot} \approx 5.1$ b $= 4\pi R'^2$, where $R' = 6.4$ fm.

IV. SYSTEMATICS OF THE RESULTS

Figure 2 is a plot of the cumulative number (N) of observed resonances for ^{113}In (lower part) and ^{115}In (upper part) vs neutron energy E. The indicated slopes, $\langle D\rangle$, were chosen visually; they do not represent actual s or p level spacings. Other considerations enter into the final determination of level spacings. For given resolution and sample thickness, the self-indication method is more sensitive for the detection of weak ($\Gamma_\gamma \gg \Gamma_n$) resonances than the transmission method. It is thus most effective for lower energies, viz, below 500 eV for indium, where not many ^{115}In s levels are missed and a significant number of p levels are seen (see below). For the remainder of the energy range (to 2 keV) the effect of resolution renders the thick sample transmission measurements equally capable of detecting levels. Many (weak) s and p levels are missed above 500 eV. The lower observed $\langle D\rangle$ indicates this effect. The masking of ^{113}In levels by ^{115}In levels at higher energies is also evident in the figure.

Figure 3 is a plot of $\sum g\Gamma_n^0$ vs energy for ^{115}In to 2004 eV. It includes the contributions from all of the 233 observed ^{115}In levels. The average slope gives $10^4 S_0 = (0.26 \pm 0.03)$ with negligible error due to some included (weak) p levels and missed s levels. The indicated uncertainty is based only on the number of s levels to 2004 eV, including missed weak s levels.

The distributions of observed $(g\Gamma_n^0)^{1/2}$ values for ^{115}In to 500 eV and to 2 keV are shown in Fig. 4. The histogram to 500 eV shows an excess of weak levels over that expected from the Porter-Thomas (P-T) single channel distribution for s levels only, assuming essentially equal $\langle g\Gamma_n^0\rangle$ for the two s populations ($J=4$ and 5). Above 500 eV, the probability of missing weak levels (first histogram box) is much larger, but the distribution to 2 keV, except for the first histogram box, is expected to not include p levels, or lack s levels having $(g\Gamma_n^0)^{1/2} > 0.25$ meV$^{1/2}$. Only the stronger levels, $(g\Gamma_n^0)^{1/2} \geq \gamma \gtrsim 0.25$ meV$^{1/2}$, were considered in choosing a proper "true" number of s population levels to 2 keV. We assume that a single channel P-T distribution applies, having the same $\langle g\Gamma_n^0\rangle$ for $J=4$ and $J=5$. For each choice of γ which is expected to yield all s levels and no p levels having $(g\Gamma_n^0)^{1/2} \geq \gamma$, a comparison was made of the observed value $M(\gamma)$ and the implied total number $N(\gamma)$ of s levels to 2 keV which would predict that $M(\gamma)$ levels will have $(g\Gamma_n^0)^{1/2} \geq \gamma$. The constraint is made that $10^4 S_0 = 0.26$. Using $\gamma = 0.25$, 0.30, and 0.35 meV$^{1/2}$ gave a best fit $N = 212$, corresponding to $\langle D\rangle = 9.4$ eV for ^{115}In. The P-T fit in Fig. 4 is excellent for the second and higher histogram boxes.

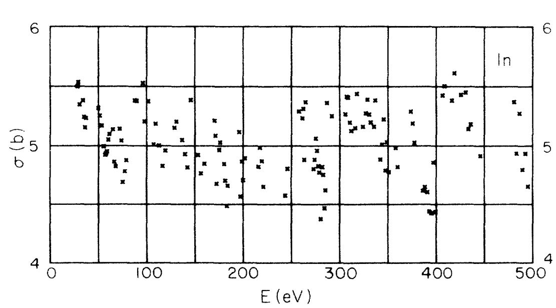

FIG. 1. The between-level total cross section vs energy for natural indium to 500 eV with sample thickness $1/n = 10.04$ b/atom. Many-channel averages were used and regions close to resonances avoided.

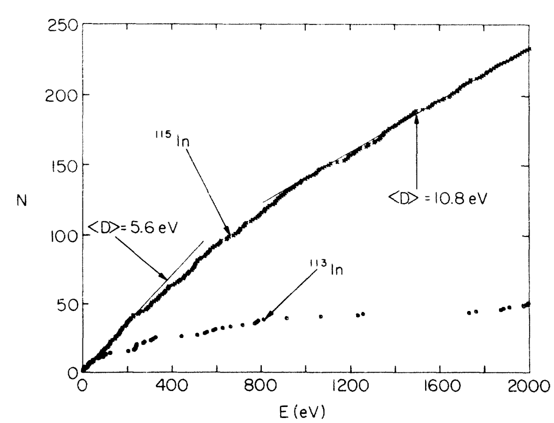

FIG. 2. Cumulative number N of observed ^{113}In (lower part) and ^{115}In (upper part) levels vs neutron energy. The values of $\langle D\rangle$ shown are slopes of the visually fitted lines; they do not represent actual $l=0$ spacings.

The next step in the analysis involves noting the value of $g\Gamma_n^0$ vs E where the probability is ~50% for detecting or missing the level. With this threshold choice, the small number of still weaker levels included should be essentially the same as the number of slightly stronger levels missed. The expected number of missed s levels is then the predicted (P-T) number of s levels having $g\Gamma_n^0 <$ this $g\Gamma_n^0(E)$ for our above choices of S_0 and $\langle D\rangle$. This analysis predicts that 4 weak s levels were missed for $E \leq 500$ eV, and 43 missed for $E \leq 2$ keV. This implies that 27 of our weak levels to 500 eV, and 64 to 2 keV, were p levels. The next step in the analysis is to find the implied value of the p strength function S_1 that would predict this result. The analysis only uses the region to 500 eV, where the p-wave detection probability is much larger than for $E > 500$ eV.

The analysis for S_1 requires that assumptions be made concerning the distribution of $g\Gamma_n^1 \equiv g\Gamma_n^0(E_1/E)$ for the ^{115}In p levels, where E_1 is the energy at which $kR = 1$ and $R = 1.40A^{1/3}$ fm is the effective nuclear radius. For $R = 6.8$ fm, this gives $E_1 = 457$ keV $\gg 2$ keV. The factor (E/E_1), where $E \ll E_1$, arises from the barrier penetration factor for p-wave neutrons. For p neutrons, we can have $J = 3, 4, 5$, or 6. If we use a mean level density proportional to $(2J+1)$, the same for s and p neutrons, there should be twice as many p levels as s levels. One approximate method of analysis assumes that a common $\langle g\Gamma_n^1\rangle$ applies for all J states with a common P-T single channel distribution for the $g\Gamma_n^1$ values. It has been suggested[14,15] that a better approach is to treat the $J=3$ and 6 states as having $g\Gamma_n^1$ values distributed according to P-T single channel theory, but to consider the $J=4$ and 5 levels as having two channel P-T distributions, where the $\langle g\Gamma_n^1\rangle$ contribution from each channel is the same for all cases, including the $J=3$ and 6 levels. If p neutron interactions are considered to be either $p_{1/2}$ or $p_{3/2}$ interactions, the $p_{3/2}$ interactions have double the statistical weight as $p_{1/2}$ or $s_{1/2}$ interactions, but may have the same $\langle g\Gamma_n^1\rangle$. Both $p_{1/2}$ and $p_{3/2}$ contribute to $J=4$ and 5, but only $p_{3/2}$ to $J=3$ or 6. The existence of two degrees of freedom in forming $J=4$ or 5, but only one in forming $J=3$ or 6 also holds if we first add $\vec{I}$ and $\vec{l}$, and later add the neutron $\vec{s}$ to the sum. An optical model with (l, s) coupling to give the split p maximum in the strength function in the region $A = 90$ to 120, places the $p_{3/2}$ maximum near the lower end and the $p_{1/2}$ maximum near the A for ^{115}In. For simplicity, however, we assume equal $\langle g\Gamma_n^1\rangle$ for each of the six channels. The equal $\langle g\Gamma_n^1\rangle$ single channel approach for $J=3,4,5,6$ (four populations), and equal $\langle g\Gamma_n^1\rangle$ for each of the six channels where $J=3$ and 6 have single channel, and $J=4$ and 5 have two channel P-T distributed net $g\Gamma_n^1$ distributions thus represent two extreme cases. For both

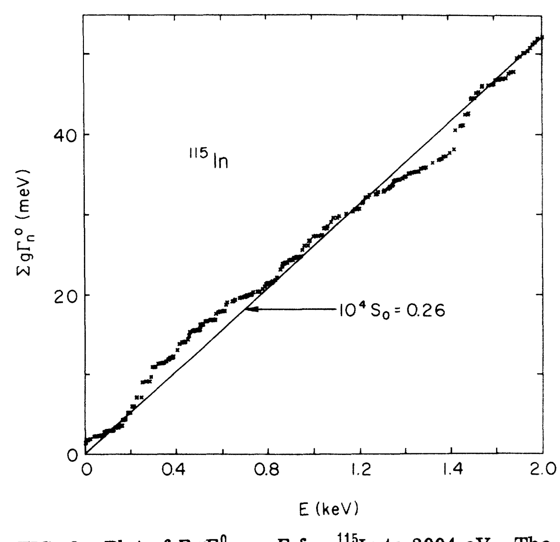

FIG. 3. Plot of $\Sigma g\Gamma_n^0$ vs E for ^{115}In to 2004 eV. The slope of the fitted straight line gives the s strength function for ^{115}In.

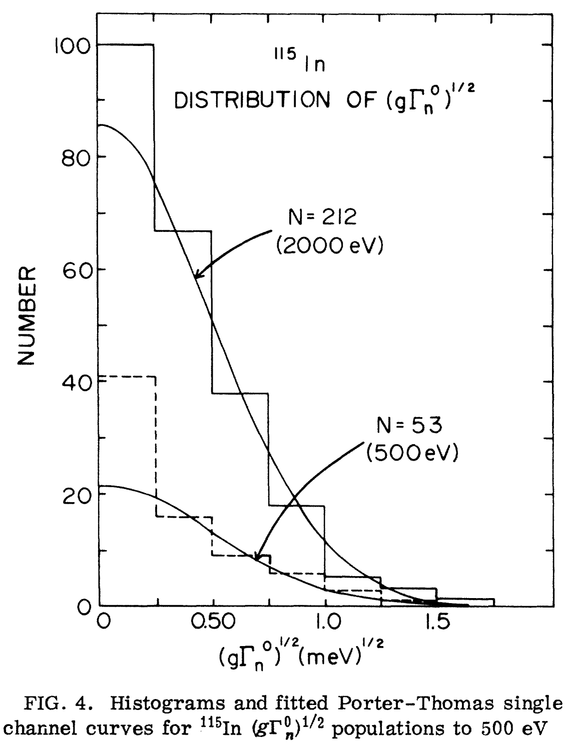

FIG. 4. Histograms and fitted Porter-Thomas single channel curves for ^{115}In $(g\Gamma_n^0)^{1/2}$ populations to 500 eV (lower part), and 2 keV (upper part). The fits are made to the data excluding the first histogram box for both energy ranges. Missing s levels and observed p levels fall into the first box. The curves are normalized to the experimental S_0 value. The values of N represent the theoretical total number of s levels for the energy intervals.

cases, a selection $10^4S_1 \approx 2.5$ predicts that ≈ 27 p levels will be observed to 500 eV. The analysis includes the reduction of the 500 eV interval by regions where stronger s or p levels in natural In would prevent the detection of such p levels (~15% of the energy interval). For the second analysis choice, values of $10^4S_1 = 1.8$ and 3.5 predict, respectively, means of ≈ 19 and 36 observed p levels.

The next analysis procedure was to use a Bayes's theorem approach[16] to establish the *a posteriori* probability for each (weak) level to be s or p. The set of 27 levels to 500 eV having the highest probability of being p levels was independent of the choice of S_1 or of the four or six channel analysis for p levels. These levels in Table II have an asterisk before the energy. Figure 5 shows the cumulative distribution of the number of these (27) levels having $g\Gamma_n^1$ values greater than the abscissa value. For comparison, we show the predicted number of p levels to 500 eV, for 85% of the energy interval not blocked by s levels. The solid curves are for $10^4S_1 = 2.5$, 3.0, and 3.5 for the six population case. The dashed curve is for the four single channel analysis using $10^4S_1 = 2.5$. It is seen that

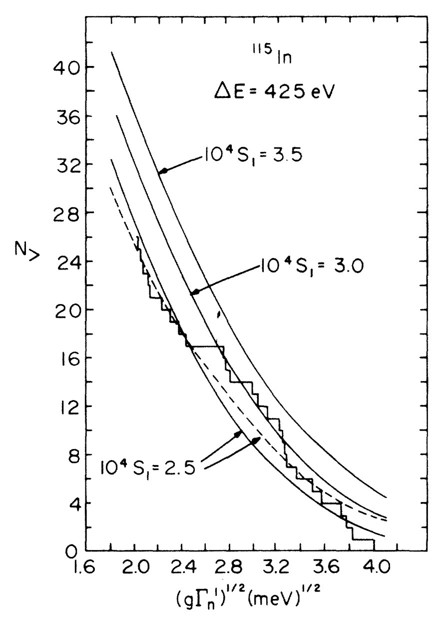

FIG. 5. Cumulative distribution of $(g\Gamma_n^1)^{1/2}$ values for those 27 ^{115}In levels to 500 eV that have greatest Bayes's theorem probability for being $l = 1$. The energy interval ΔE is 500 eV minus the portion masked by strong s levels. The dashed curve is the integral Porter-Thomas distribution assuming all four J states have a common $\langle g\Gamma_n^1\rangle$ and have single channel P-T distributions for $(g\Gamma_n^1)^{1/2}$. The solid curves refer to the case where $J = 3$ and 6 have single channel P-T distributions, but $J = 4$ and 5 have two-channel distributions — with all channels having equal $\langle g\Gamma_n^1\rangle$. The curves are normalized to the p strength functions indicated in the figure.

the portion above $(g\Gamma_n^1)^{1/2} = 2.7$ meV$^{1/2}$ favors a higher choice 10^4S_1 than the full region above $(g\Gamma_n^1)^{1/2} = 2.0$ meV$^{1/2}$. This probably indicates a lower probability of detecting the weaker p levels. We also note that ~1 to 4 p levels having $(g\Gamma_n^1)^{1/2}$ >4.1 meV$^{1/2}$ are predicted for 10^4S_1 from 2.5 to 3.5, while the Bayes's analysis would place any such exceptionally strong p level with the s level grouping. The over-all conclusion from the analysis is that $10^4S_1 = 2.7 + 1.0$ or -0.7. This is consistent with the recent determination by Camarda[17] of $10^4S_1 = (3.15 \pm 0.6)$ based on energy dependence of the average total cross section vs energy for $E = 1$ to 600 keV. Since S_1 is expected to have some energy dependence even in the absence of intermediate structure effects, the "true" value for $E \leq 500$ eV need not be the same as the average from 1 to 600 keV.

Our final analysis involves comparing with theory the resulting s population to 500 eV, after removing the 27 levels most apt to be $l = 1$. These 49 levels should have 4 "missed" weak s levels added from the preceding tests of the expected number of missed weak s levels to 500 eV, for 53 s levels altogether. For the 49 levels, the value of the experimental Dyson-Mehta Δ statistic[1] is 1.36 vs (0.63 ± 0.22) predicted. The value of Δ is the mean

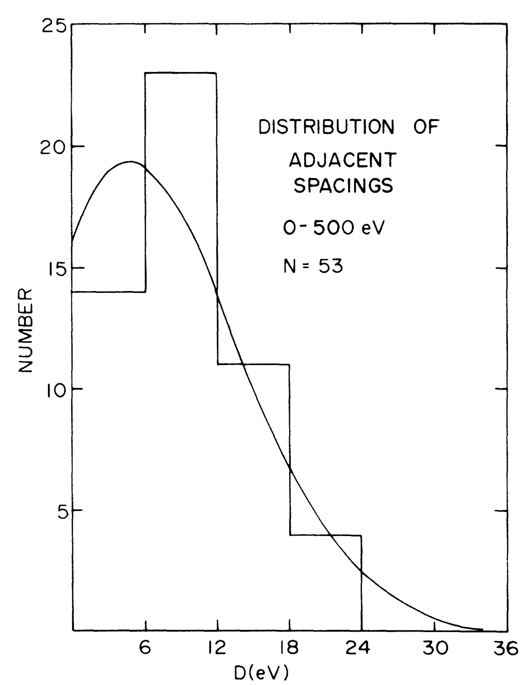

FIG. 6. ^{115}In nearest neighbor spacing histogram and Wigner two-population spacing distribution for 49 observed (and probably $l = 0$) levels plus four levels inserted at the midpoints of the four largest spacings (to compensate for the predicted loss of four s levels to 500 eV).

square deviation of the N vs E histogram from a best fit straight line. The 49 levels include 4 levels to 12.1 eV, 13 levels (0–100) eV, and 10, 8, and 9 levels, respectively, for the next 100 eV intervals.

If we add levels at 238, 277, and 307 eV, near the centers of the largest nearest neighbor spacing intervals of 23.4, 21.9, and 25.2 eV, respectively, the "experimental" $\Delta = 0.57$ vs (0.65 ± 0.22) from theory. The next three largest nearest neighbor spacing intervals are all 20 to 21 eV and are centered near 104, 330, and 488 eV. Adding just one of these at a time to the 238, 277, and 307 eV levels gives experimental Δ values of 0.76, 0.40, and 0.56, respectively, vs $\Delta_{D\text{-}M} = (0.65 \pm 0.22)$ and 1.04 for a set of uncorrelated Wigner spacings. The resulting sets of 53 s levels to 500 eV show how the choice of a single level can influence "Δ_{exp}." The comparison does not, however, represent a serious test of the theory, for which the results for ^{166}Er, ^{182}W, and other even A rare earth isotopes give much more convincing tests.[1-5] Figure 6 shows the nearest neighbor spacing histogram resulting from the placing of four levels at the midpoints of the four largest observed spacings. The theoretical curve is the Wigner two-population distribution for 53 levels and for target spin $\frac{9}{2}$. Insertion of the four levels tends artificially to raise the center part of the histogram. Otherwise, the fit is quite good.

We thank Dr. H. Ceulemans for his involvement in the operations to obtain the data, and Dr. C. Coceva for sending us his results on neutron capture in separated ^{113}In and natural indium. The technical support of L. Morganstein, W. Van Wart, and the late A. Blake is gratefully acknowledged. Dr. G. Rogosa of the U. S. Atomic Energy Commission provided essential help in procuring the separated isotope sample.

---

†Research supported by the U. S. Atomic Energy Commission.

*Present address: Lawrence Livermore Laboratory, Livermore, California 94550.

‡Present address: Burns and Roe, Oradell, New Jersey 07649.

§Present address: New Jersey Department of Higher Education, Trenton, New Jersey.

‖Present address: University of Capetown, Capetown, Union of South Africa.

[1]H. I. Liou *et al.*, Phys. Rev. C 5, 974 (1972), Er.

[2]F. Rahn *et al.*, Phys. Rev. C 6, 251 (1972), Sm, Eu.

[3]F. Rahn *et al.*, Phys. Rev. C 6, 1854 (1972), ^{232}Th, ^{238}U.

[4]H. I. Liou *et al.*, Phys. Rev. C 7, 823 (1973), Yb.

[5]H. S. Camarda *et al.*, Phys. Rev. C 8, 1813 (1973), W.

[6]F. Rahn *et al.*, Phys. Rev. C 8, 1827 (1973), Na.

[7]U. N. Singh *et al.*, Phys. Rev. C 8, 1833 (1973), K.

[8]H. I. Liou *et al.*, Phys. Rev. C 10, 709 (1974), Cd.

[9]*Neutron Cross Sections*, compiled by M. D. Goldberg, S. F. Mughabghab, S. N. Purohit, B. A. Magurno, V. M. May, Brookhaven National Laboratory Report No. BNL-325 (National Technical Information Service, Springfield, Virginia, 1966), 2nd ed., 2nd Suppl. Vol. IIB, $Z = 41-60$. J. A. Harvey *et al.*, Phys. Rev. 99, 10 (1955); V. L. Sailor and L. B. Borst, *ibid.* 87, 161 (1952).

[10]C. Coceva, private communication. See also Euratom Internal Report, Geel No. 30, 1972, (unpublished), p. 22. Spin assignments for 32 levels in ^{115}In are given in a paper by F. Corvi and M. Stefanon, Nucl. Phys. (to be published).

[11]C. Coceva *et al.*, Phys. Rev. Lett. 25, 1047 (1970).

[12]G. Hacken *et al.*, Bull. Am. Phys. Soc. 14, 496 (1969).

[13]*Neutron Cross Sections*, compiled by S. F. Mughabghab and D. I. Garber, Brookhaven National Laboratory Report No. BNL-325 (National Technical Information Service, Springfield, Virginia, 1973), 3rd ed., Vol. 1.

[14]R. E. Chrien, private communication.

[15]M. Gyulassy, R. J. Howerton, and S. T. Perkins, UCRL Report No. 50400, 1972 (unpublished), Vol. 11, p. 456.

[16]L. M. Bollinger and G. E. Thomas, Phys. Rev. 171, 1293 (1968).

[17]H. S. Camarda, Phys. Rev. C 9, 28 (1974).